

Support information

Peroxymonosulfate activation by ultra-dispersed Co_3O_4 nanosheets for efficient 4-nitrophenol degradation

S 2.4. Evaluation of catalytic performance

The 300 W Xenon lamp was used in the whole photocatalytic degradation. Briefly, 20 mg of the catalyst was added into 40 mg/L of 4-NiP solution with magnetic stirring in the dark box for adsorption equilibrium (30 min). Additionally, the 1 mmol of PMS was added into above solution to initiate the reaction under visible light irradiation. At 1 min interval, 3 mL of 4-NiP solution was withdrawn with disposable syringe and separated immediately with the 0.22 μm polytetrafluoroethylene film. The concentrations of 4-NiP were detected by the ultraviolet-visible spectrum. The contribution of the reactive oxygen species was further evaluated by the free radical trapping experiments. IPA, VC, MeOH and L-His were used as scavengers. In the electron paramagnetic resonance (EPR) experiments, 5,5-dimethyl-1-pyrroline-N-oxide (DMPO) and 2,2,6,6-tetramethyl-4-piperidone (TEMP) were applied as the spin-trapping agent for $\text{SO}_4^{\cdot-}$, $\cdot\text{OH}$, $\text{O}_2^{\cdot-}$ and $^1\text{O}_2$, respectively. The deionized water, tap water, river water and reservoir water were used to evaluate the applications of catalyst in approximate real wastewater. Furthermore, the effect of inorganic anions (Cl^- , HCO_3^- , CO_3^{2-} , NO_3^- , SO_4^{2-} , H_2PO_4^- and HPO_4^{2-}) on removal efficiency of 4-NiP were investigated. The catalytic degradation of four kinds of antibiotics mixture (20 mg/L for 4-NiP, 2C4Nip, 2C6Nip, TC, OTC, DOX, CIP, MR, MB, and MO, respectively) was investigated with the same methods. The degradation percentage was calculated by the intensity of characteristic absorption peak. The water quality analysis report was obtained from Hangzhou Yanqu Information Technology Co., Ltd. The EPR signals was measured to further identify the contribution of different reactive oxygen species (ROSs). The intermediates of 4-NiP were identified by liquid chromatography-mass (LC-MS, Agilent LC1290-QQQ-6490, USA). The experiments were repeated three times in the same procedure, and which were depicted with mean values and the error bar.

S 2.5. Computational details

Density functional theory calculations were performed utilizing the Vienna Ab initio Simulation Package with the projector augmented wave method. The exchange-correlation interactions were treated using the spin-polarized Perdew-Burke-Ernzerhof functional. $A_2 \times 2 \times 1$ supercell model of Co_3O_4 was constructed by combining the (111), (220) and (311) crystal plane.

All computations were conducted under spin-polarized conditions. A plane-wave basis set with a cutoff energy of 450 eV and appropriate k-point meshes were employed to ensure convergence of the total ground-state energy. Structural optimizations were performed until the forces on all relaxed atoms were below $0.02 \text{ eV} \cdot \text{\AA}^{-1}$. For optimizing both geometry and lattice parameters, Brillouin zone integration was carried out using a $2 \times 2 \times 1$ Gamma-Pack k-point grid. A denser $1 \times 1 \times 1$ Gamma-Pack k-point sampling was adopted for density of states calculations. The energy convergence threshold for self-consistent field iterations was set to 10^{-5} eV during structural relaxation. Equilibrium geometries and lattice constants were obtained when the maximum stress on any atom fell below $0.02 \text{ eV} \cdot \text{\AA}^{-1}$. Input and output files for elastic modulus calculations,

including charge density differences, were managed using the VASPKIT toolkit.

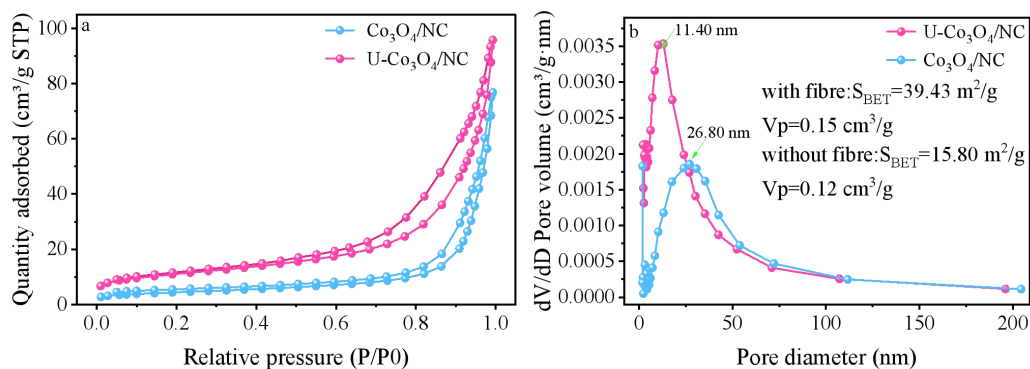


Fig. 1S. (a) N₂ adsorption/desorption isotherms and (b) pore size distribution of the U-Co₃O₄/NC and Co₃O₄/NC.

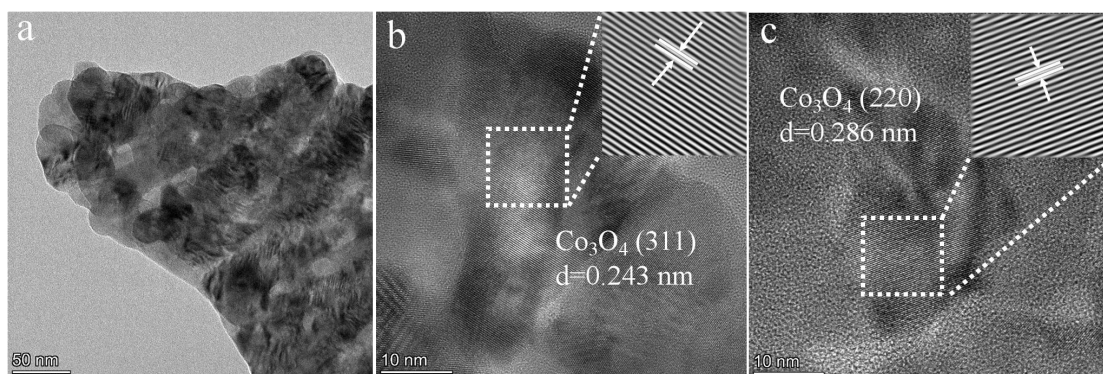


Fig. 2S. (a) SEM and (b-c) TEM images of Co₃O₄/NC catalysts.

Table 1S. The degradation efficiency of the selected organic pollutants in different water matrices.

Name	Degradation rate (%)			
	De-W	Ta-W	Re-W	Ri-W
DOX	96.67	95.07	98.82	91.31
TC	99.93	99.73	98.48	92.32
OTC	98.49	97.87	98.89	97.90
4-NiP	98.08	96.76	94.37	90.88
2C6NiP	98.40	99.58	99.37	99.63
2C4NiP	99.82	99.51	99.94	99.57
MB	99.71	99.69	99.87	99.75
MO	99.93	99.24	99.43	99.81
MR	98.88	99.56	98.83	99.53